

Safety and chronic lesion characterization of pulsed field ablation in a Porcine model

Mark T. Stewart BS¹  | David E. Haines MD, FHRS² | Damijan Miklavčič PhD³ | Bor Kos PhD³ | Nicole Kirchhof DVM¹ | Noah Barka DVM¹ | Lars Mattison PhD¹ | Matt Martien MS¹ | Birce Onal PhD¹  | Brian Howard PhD¹ | Atul Verma MD, FHRS⁴ 

¹Cardiac Rhythm Management, Medtronic, Inc., Minneapolis, Minnesota, USA

²Beaumont Health System, Div of Cardiology, EP Services, Oakland University William Beaumont School of Medicine, Royal Oaks, Michigan, USA

³Faculty of Electrical Engineering, University of Ljubljana, Ljubljana, Slovenia

⁴Southlake Regional Health Centre, Arrhythmia Services, University of Toronto, Newmarket, Ontario, Canada

Correspondence

Mark T. Stewart, Cardiac Rhythm Management, Medtronic, Inc, 8200 Coral Sea St, N.E., Minneapolis, MN 55112.
Email: mark.stewart@medtronic.com

Funding information

Medtronic Inc.

Abstract

Background: Pulsed field ablation (PFA) has been identified as an alternative to thermal-based ablation systems for treatment of atrial fibrillation patients. The objective of this Good Laboratory Practice (GLP) study was to characterize the chronic effects and safety of overlapping lesions created by a PFA system at intracardiac locations in a porcine model.

Methods: A circular catheter with nine gold electrodes was used for overlapping low- or high-dose PFA deliveries in the superior vena cava (SVC), right atrial appendage (RAA), and right superior pulmonary vein (RSPV) in six pigs. Electrical isolation was evaluated acutely and chronic lesions were assessed via necropsy and histopathology after 4-week survival. Acute and chronic safety data were recorded peri- and post-procedurally.

Results: No animal experienced ventricular arrhythmia during PFA delivery, and there was no evidence of periprocedural PFA-related adverse events. Lesions created in all anatomies resulted in electrical isolation postprocedure. Lesions were circumferential, contiguous, and transmural, with all converting into consistent lines of chronic replacement fibrosis, regardless of trabeculated or smooth endocardial surface structure. Ablations were non-thermally generated with only minimal post-delivery temperature rises recorded at the electrodes. There was no evidence of extracardiac damage, stenosis, aneurysms, endocardial disruption, or thrombus.

Conclusion: PFA deliveries to the SVC, RAA, and RSPV resulted in complete circumferential replacement fibrosis at 4-week postablation with an excellent chronic myocardial and collateral tissue safety profile. This GLP study evaluated the safety and efficacy of a dosage range in preparation for a clinical trial and characterized the non-thermal nature of PFA.

KEYWORDS

atrial fibrillation, catheter ablation, electroporation, pulsed electric field modeling, pulsed field ablation

[Correction added on March 23, 2021, after first online publication: the figure 2 has been revised and corrected.]

This is an open access article under the terms of the Creative Commons Attribution-NonCommercial-NoDerivs License, which permits use and distribution in any medium, provided the original work is properly cited, the use is non-commercial and no modifications or adaptations are made.

© 2021 The Authors. *Journal of Cardiovascular Electrophysiology* published by Wiley Periodicals LLC

1 | INTRODUCTION

It is estimated that 33 million individuals worldwide have atrial fibrillation (AF) with continued growth due to an aging demographic.^{1,2} Pulmonary vein isolation by catheter ablation is a proven therapy for the treatment of patients with AF, and radiofrequency (RF) is a widely used thermal energy source for the ablation procedure.^{3,4} RF catheter ablation can be effective in treating AF patients with long-term maintenance of sinus rhythm ranging from 53% to 79.8%.^{5–9} RF technology relies on thermal conduction for lesion formation, which is dependent on adequate contact between the RF electrode and the targeted tissue.^{10–13} Moreover, ablation of a thicker wall or trabeculated regions in the atria has proven challenging, and current thermal ablation technologies are limited to avoid damage to collateral structures, such as the phrenic nerve.^{14,15}

Based on cell membrane irreversible electroporation (IRE), pulsed field ablation (PFA) has been identified as a potential alternative to existing ablation technologies.^{16–23} PFA delivery is not reliant on uniform electrode-tissue contact for lesion creation, and can ablate myocardial cells without collateral tissue damage which may enhance the safety profile of this energy source.^{24–27} Currently, no preclinical study has evaluated the potential for adverse effects from repeated overlapping energy deliveries on the same targeted local myocardium, nor provided a detailed analysis of the non-thermal aspect of PFA based on electrode temperature recordings. Consequently, the aim of this Good Laboratory Practices (GLP) study was to evaluate the safety of a PFA system analogous to the system planned to be used first-in-human study by assessing the safety and chronic characteristics of lesions created from overlapping PFA deliveries. This is the first study to establish safety and efficacy of overlapping PFA deliveries using two applied voltage levels on tissues of varying thickness (right superior pulmonary vein [RSPV], superior vena cava [SVC], left atrial appendage). This GLP study set the stage for voltage levels used in human clinical trials and characterized the non-thermal nature of PFA deliveries.

2 | METHODS

2.1 | Preclinical study design

This GLP animal study evaluated the safety and chronic lesion characterization of overlapping deliveries using a PFA system prepared for clinical use. A previously described initial feasibility PFA system was reported²⁴; however, this preclinical study evaluated a distinct PFA system²⁸ prepared for usage in a first-in-human clinical study. The study was conducted at Medtronic's Physiological Research Laboratory that is certified by the Association for Assessment and Accreditation of Laboratory Animal Care. The protocol was approved by the Institutional Animal Care and Use Committee and conformed to the Guide for the Care and Use of Laboratory Animals. This GLP study was completed before any human studies.

Six female Yorkshire pigs (age 3.4–5.0 months and 59–70 kg body weight at the time of ablation) underwent intracardiac PFA via femoral vein access while maintained under isoflurane (1.0%–2.8%) anesthesia. Amiodarone (150 mg IV) was administered before ablations and heparin (175–300 units/kg IV) was infused to maintain an activated clotting time of at least 350 s. Prophylactic antimicrobial drugs (cefazolin 22.5 mg/kg IV and amoxicillin 10 mg/kg PO) were administered. Analgesic control was assessed daily for three days postoperatively and managed with transdermal fentanyl (150 mcg per hour), local bupivacaine (50 mg), buprenorphine (0.01 mg/kg SQ) and carprofen (4 mg/kg PO).

2.2 | PFA modeling

A three-dimensional model of the RSPV was constructed based on contrast enhanced computed tomography images of a single pig. Heart segmentation and surface reconstruction was done using Mimics (Materialize). To accommodate realistic placement of the ablation catheter, the inner surface of the RSPV was extended outward by surface modification using 3-matic (Materialize). The RSPV wall was reconstructed using a uniform 3 mm thickness to simulate the actual RSPV average tissue thickness in the study animals. The catheter electrode segments were positioned in four placements with the shape of the circular catheter conforming to the inner surface of the RSPV ostium, while the RSPV was extended to a more circular shape. The numerical model was then solved for the electric potential using the Laplace equation while taking into account the electric field-dependent increase in conductivity using Comsol Multiphysics (Comsol AB).²⁹ The resulting electric field strength was exported into Matlab (Mathworks), which was used to generate the electric field iso-surfaces at a conservative field threshold of 550 V/cm for lesion creation.³⁰ The electric field isosurfaces (representing the extent of ablated tissue volume) were then used to generate the final lesion reconstruction in 3-matic. A lower IRE field threshold value of 400 V/cm has been commonly cited for cardiomyocytes.²⁵

2.3 | Catheter ablation and PFA dosing

The SVC, muscle sleeve portion; low dose of ± 700 V), right atrial appendage (RAA) (dose of ± 1500 V), which was chosen as a structure with trabeculated anatomy which could be targeted for electrical isolation, and RSPV (high dose of ± 1500 V) were targeted with PFA (Figure 1). A nine-electrode circular array pulmonary vein ablation catheter (PVAC GOLD; Medtronic), powered by a custom-built PFA research generator, was used to deliver bipolar biphasic PFA pulses. In contrast to a prior publication,²⁴ the PFA generator and delivery catheter used in this study are analogous to the PFA system planned to be used clinically (clinicaltrials.gov, NCT04198701).²⁸ This study was performed before the initiated human clinical trial.

For PFA applications, the generator delivered trains of short, low or high voltage, biphasic pulses to the PVAC GOLD catheter (without

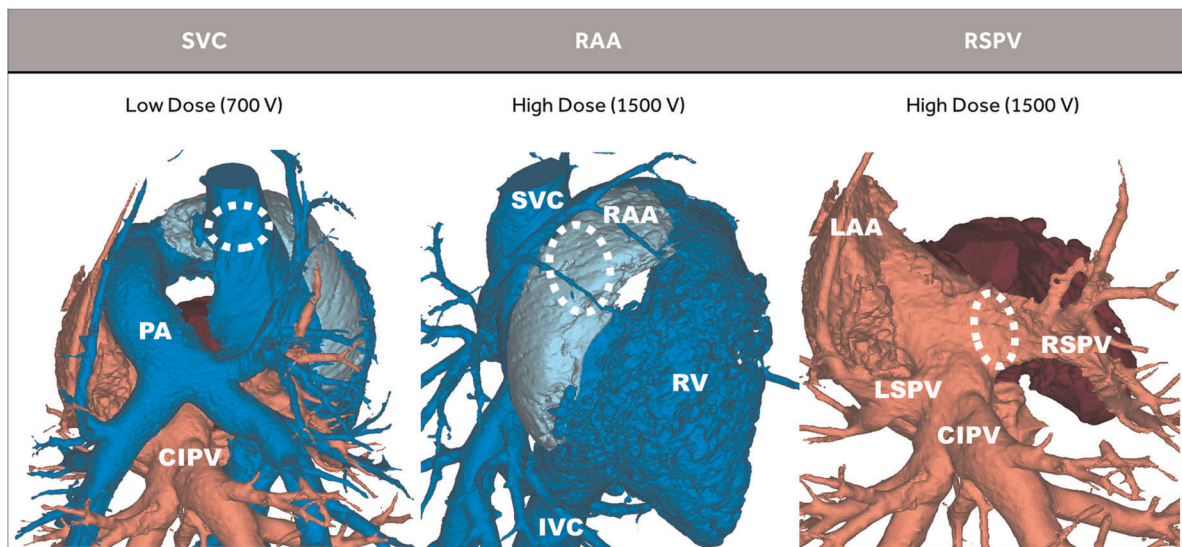


FIGURE 1 Porcine model summary. In six pigs, a low (± 700 V) dose of pulsed field ablation (PFA) was delivered to the superior vena cava (SVC) (muscle sleeve portion), and a high (± 1500 V) dose of PFA was delivered to the right atrial appendage (RAA), and right superior pulmonary vein (RSPV). The common inferior pulmonary vein (CIPV) was not ablated

the use of a patient return electrode patch) through a bipolar delivery system that connects alternating electrodes as opposing polarities. The PFA system was connected to a cardiac R-wave monitor (Model 7700; Ivy Biomedical) to gate pulse train deliveries and PFA dosing was based on the expected thickness of the targeted tissue and previous experimental observations.²⁴ Concurrent with all deliveries of PFA therapy, temperature change was measured on each electrode to characterize the potential for thermal effects. Specifically, temperature recordings were measured at baseline, and within approximately 1 s of the end of each pulse train delivery.

The experimental protocol began with low dose PFA applications to the SVC, in consideration that the expected myocardial thickness would be less than one millimeter and the right phrenic nerve (RPN) would be within 1 or 2 mm from the electrode array. Before energy delivery, the circular array catheter was moved into the cranial aspect of the SVC and a minimum bipolar phrenic nerve pace stimulation threshold was established. The catheter was repositioned on the muscle sleeve near the right atrial junction. Pulse trains which consisted of a series of biphasic pulses, each of these having a +700 V pulse followed by a reverse polarity -700 V pulse, were delivered to the muscle sleeve with four overlapping placement sites of the catheter and four pulse trains delivered per each placement. The catheter placement intent was to expose the targeted myocardial sleeve and surrounding collateral tissue to the PFA deliveries with significant overlap of the 16 pulse trains. The circular array catheter was moved to the distal muscle sleeve and electrical isolation was checked postablation. The phrenic nerve function was also rechecked for stimulation threshold in the cranial location. SVC muscle sleeve isolation and phrenic nerve threshold were checked four weeks later at the study termination procedure.

The high PFA dose (trains consisting of a series of biphasic pulses, each of these having +1500 V pulse followed by -1500 V

pulse) was used during ostial RAA and RSPV ablations to study the safety and efficacy of lesion creation in clinically relevant targets^{3,4,15} to evaluate the effects of high amplitude and overlapping PFA deliveries. The circular array catheter was placed eight times each at the orifice of the RSPV and just within the ostium of the RAA and four pulse trains were delivered at each of the eight sites. Like SVC deliveries, the objective was to expose the targeted myocardium and surrounding tissue to multiple overlapping ablations (32 total pulse trains in these sites). This ablation method was performed to evaluate the effect of overlapping deliveries on collateral damage and targeted myocardium. Electrical isolation was finally evaluated acutely at all sites using the ablation catheter.

After the ablation procedure, each pig was recovered under veterinary supervision. Enoxaparin 60 mg IV twice daily was administered for anticoagulation, with clopidogrel 75 mg PO once daily as an alternative if venous access was not available. Animals were survived for four weeks, euthanized, and underwent gross and microscopic pathology evaluation. To aid in lesion visualization, an IV infusion of 20 ml of a 10% solution of triphenyl tetrazolium chloride was delivered intravenously, five minutes before euthanasia. All animals were clinically normal until their scheduled euthanasia on day 28 post ablation.

2.4 | Pathology

Pathology assessments were completed by a board-certified veterinary pathologist experienced in device pathology. At necropsy, ablation sites were comprehensively evaluated, and ablation lesions visually documented. All tissues were then fixed in 10% neutral buffered formalin and subsequently re-examined via backlight illumination, and trimmed. One complete atrial cross section or select

tissue areas (e.g., representative lesions or areas of uncertain ablation success from a longitudinally incised SVC) were dehydrated, paraffin embedded, and sectioned at approximately 3–5 μm . Two serial sections per paraffin block were stained with hematoxylin and eosin and with Masson's trichrome. Slides were assessed via brightfield microscopy for the following parameters: (1) lesion transmural, (2) maximum thickness of the ablated tissue now presenting as ablation fibrosis, (3) thickness of adjacent unablated cardiac tissues, (4) gaps (surviving myofibers) within the ablation fibrosis, (5) evaluation for intralesional inflammation, (6) calcification, (7) neointimal formation, and (8) any other pathological changes that could present an impediment to the safety profile. Gross and histopathological observations were combined to decide on the morphological/anatomical ablation outcome.

3 | RESULTS

3.1 | Acute safety and electrical isolation of SVC ablation

None of the animals experienced ventricular arrhythmia during or after any of the PFA deliveries and there was no indication of acute injury to collateral structures. Phrenic nerve (diaphragm) stimulation was observed during 94 of 96 PFA pulse train deliveries in the SVC and during 188 of 192 PFA pulse train deliveries in the RPV and 190 of 194 deliveries in the RAA without affecting acute or chronic phrenic nerve function. Bipolar pace stimulation thresholds (Table 1) for the RPN tested pre-ablation, immediately Postablation, post-procedure, and at the 28 days euthanasia timepoint using 0–10 V bipolar pacing averaged 0.42 ± 0.21 , 0.48 ± 0.29 , 0.40 ± 0.21 , and 0.48 ± 0.25 V, respectively. Local electrograms were immediately reduced after the first pulse train delivery for each of the targeted sites (Figure 2). Regarding the dosing of each tissue site with four pulse trains, there was evidence of remnant potentials after the initial ablation pulse train but after completion of all four deliveries, only far-field signals remained (Figure 2). At the end of the acute procedure, isolation of all structures was confirmed by entrance block (Figure 2). During the ablation procedure, the temperature rise was recorded and compiled from all of the electrodes one second after each pulse train during all of the overlapping ablations at each of the three tissue sites. The average temperature rise (recorded within 1 s after a ± 700 V pulse train delivery at the SVC) was

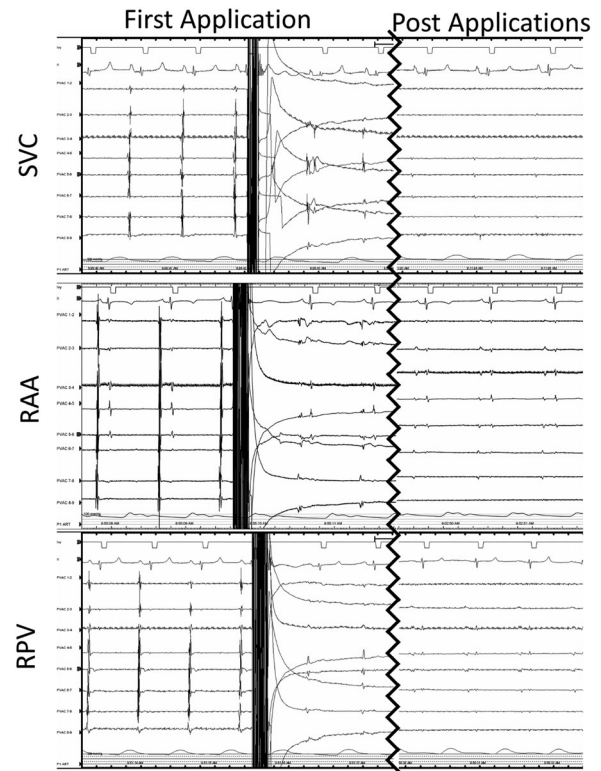


FIGURE 2 Acute Isolation of the SVC, RAA, and RSPV. Immediately after the first pulse train delivery, electrograms for each of the targeted sites were reduced and after all four pulse trains were delivered, only far-field signals remained. Complete electrical isolation of all structures was confirmed by entrance block. Entrance and exit block were confirmed for the SVC. RAA, right atrial appendage; RSPV, right superior pulmonary vein; SVC, superior vena cava

$0.70 \pm 0.35^\circ\text{C}$. The average temperature rises recorded within 1 s after a ± 1500 V delivery at the RAA and RSPV were $5.00 \pm 1.83^\circ\text{C}$ and $4.95 \pm 2.52^\circ\text{C}$, respectively. All electrodes were free of thermal deposits (coagulum) at the end of the procedures.

3.2 | Chronic lesions after ablation of the superior vena cava

All low-dose PFA deliveries resulted in morphologically complete SVC lesions based on gross and histological observations. All PFA

TABLE 1 Phrenic nerve pacing threshold summary

| Timepoint | Phrenic nerve pace stimulation threshold (Volts) | | | | | | Avg (STD) |
|----------------------|--|-------|-------|-------|-------|-------|---------------------|
| | Pig-1 | Pig-2 | Pig-3 | Pig-4 | Pig-5 | Pig-6 | |
| Pre-ablation | 0.8 | 0.2 | 0.3 | 0.4 | 0.5 | 0.3 | 0.42 (± 0.21) |
| Postablation | 0.9 | 0.2 | 0.3 | 0.8 | 0.4 | 0.3 | 0.48 (± 0.29) |
| End of procedure | 0.8 | 0.2 | 0.3 | 0.4 | 0.4 | 0.3 | 0.40 (± 0.21) |
| 28 Days postablation | 0.6 | 0.6 | 0.8 | 0.1 | 0.5 | 0.3 | 0.48 (± 0.25) |

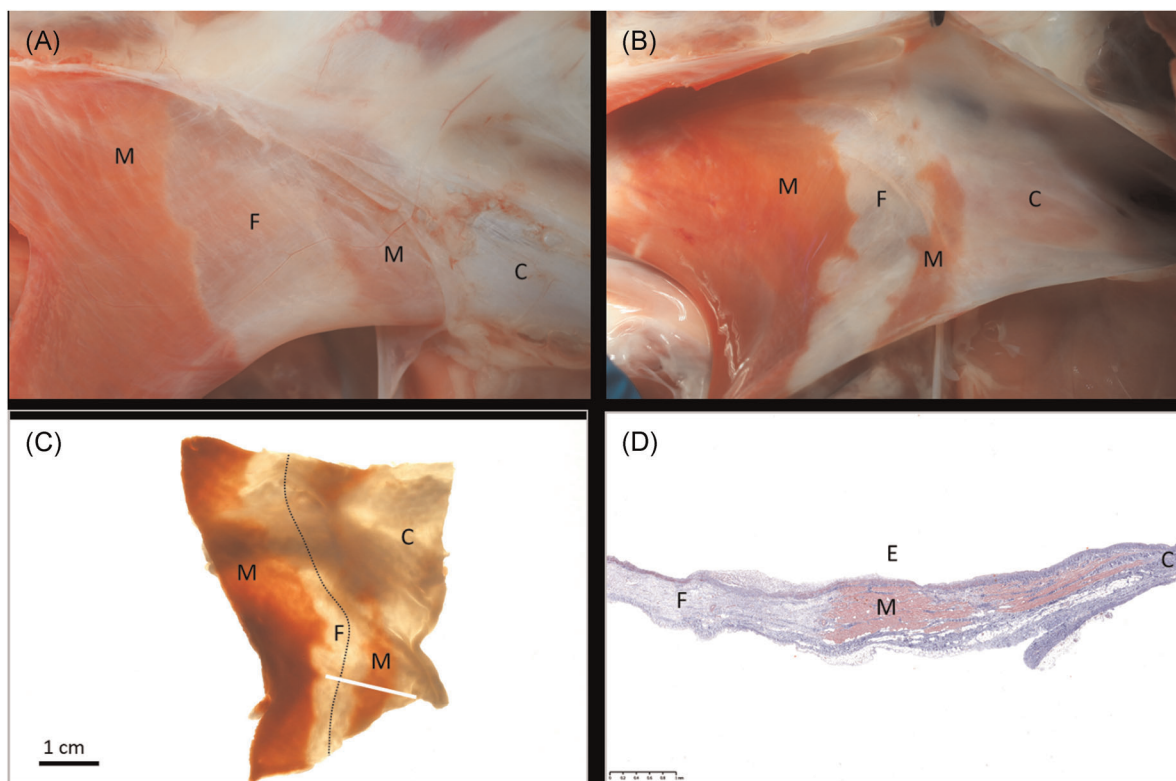


FIGURE 3 Ablation of the SVC. In-situ necropsy finding, enhanced by triphenyl tetrazolium chloride (TTC) staining, 4 weeks after low-dose PFA treatment of the SVC before (A) and after (B) opening the lumen. A continuous ablation line (dotted line) is readily visible under backlight illumination of the same specimen after formalin fixation (C). Histology confirms transmural replacement fibrosis and shows abrupt transition to normal, nontreated muscle via Masson's trichrome staining. White bar in (C) indicates slide origin for (D). C, collagenous portion of the SVC; E, endothelial side; F, fibrosis after ablation; M, muscle (untreated); PFA, pulsed field ablation; SVC, superior vena cava

deliveries to the muscular sleeves of the SVCs presented as easily discernable chronic circumferential lesions (Figure 3A,B). In more detail, the chronic lesions were approximately 1-cm wide fibrotic bands with some scalloped edges (Figure 3A) but without strictures or other evidence of lumen reduction, and without adventitial changes. Backlight illumination (Figure 3C) was highly suggestive of lesion transmural as it showed uninterrupted translucency along the ablation; this assumption was ultimately confirmed by histology (Figure 3D).

Histopathology of the SVC's ablation sites showed transmural replacement fibrosis of the muscular sleeve (measuring on average 0.47 ± 0.15 mm in ablated wall thickness, Table 2) and minor overlying neointimal formation. The transition zone from ablated to normal tissue (Figure 3D) was narrow. Pathology examination of the SVC's did not detect any remaining myofiber conduits across the postablation fibrosis.

3.3 | Chronic lesions after ablation of the right atrial appendage

All high-dose PFA applications of the RAA resulted in wide, contiguous, circumferential, and transmural lesions in all animals.

Specifically, widespread replacement fibrosis was observed around the orifice (Figure 4A) and throughout the trabeculation, regardless of its thickness (Figure 4B). Fixed tissue inspection via backlight illumination did expose diffuse atrial translucency, and it was estimated that in all animals over 50% of each RAA wall was fully ablated (Figure 4C).

Via histology, wide-ranging, circumferential, transmural replacement fibrosis measuring on average 1.29 ± 0.41 mm in wall thickness was observed in each of the single cross sections made from the RAA's (Table 2 and Figure 4D). Additional histopathological findings of the treated atrial locations comprised of mild concurrent neointimal formation but absence of thrombus, with no epicardial fat tissue inflammation, and no vascular changes (Figure 4D).

3.4 | Chronic lesions after ablation of the right superior pulmonary vein

The complete ostial circumference of each RSPV (high-dose PFA) showed fibrotic replacement of the local myocardium but no evidence of mural thrombus or grossly notable venous stenosis (Figure 5A,B). Furthermore, backlight illumination suggested that lesions were not only transmural but this technique also yielded no evidence of surviving intramural muscular tissue (Figure 5C).

TABLE 2 Pathology summary

| Targeted anatomical location | SVC | RAA | RSPV |
|--|-------------------------------|-------------------------------|--|
| Therapy profile | Low dose (700 V) | High dose (1500 V) | High dose (1500 V) |
| Number of ablated locations (n, total) | 6 | 6 | 6 |
| Continuous transmuralty achieved | 6/6 | 6/6 | 6/6 |
| Wall thickness in chronic ablation lesion, average (mm) \pm of maximum measurements of all slides SD | 0.47 \pm 0.15 (0.232–0.751) | 1.29 \pm 0.41 (0.673–2.169) | 2.62 \pm 1.56 ^c (0.524–6.514) |
| Wall thickness of adjacent unablated (native) tissue, average (mm) \pm SD | 0.53 \pm 0.23 (0.227–1.017) | 1.76 \pm 0.92 (0.792–3.668) | 2.16 \pm 1.32 (0.962–4.652) |
| Presence of viable myofibers creating cross-lesional conduits | 0/6 | 0/6 | 0/6 |
| Additional intralesional observations beyond expected healing ^a | 0/6 | 0/6 | 0/6 |
| Ablation is complete based on gross and histological observations (n/n) ^b | 6/6 | 6/6 | 6/6 |
| Average temperature rise recorded 1 s post-delivery | 0.70 \pm 0.35°C | 5.00 \pm 1.83°C | 4.95 \pm 2.52°C |

Abbreviations: RAA, right atrial appendage; RSPV, right superior pulmonary vein; SVC, superior vena cava.

^aExpected or typical myocardial remodeling after an ablation treatment 4-week earlier will result in a bulk of uniform replacement fibrosis extending from the application surface into the myocardial wall. The chronic fibrotic tissue will be devoid of major inflammation, calcification, or significant vascular or epicardial/adventitial changes. In cases of endocardial treatments, minor neointima formation is expected.

^bAn ablation is morphologically denoted as “complete” when it is circumferentially transmural along an orifice or around a tubular structure.

^cAll six RSPV ablations extended into right atrial tissues, extending the lesion depths into this adjoining atrial myocardium.

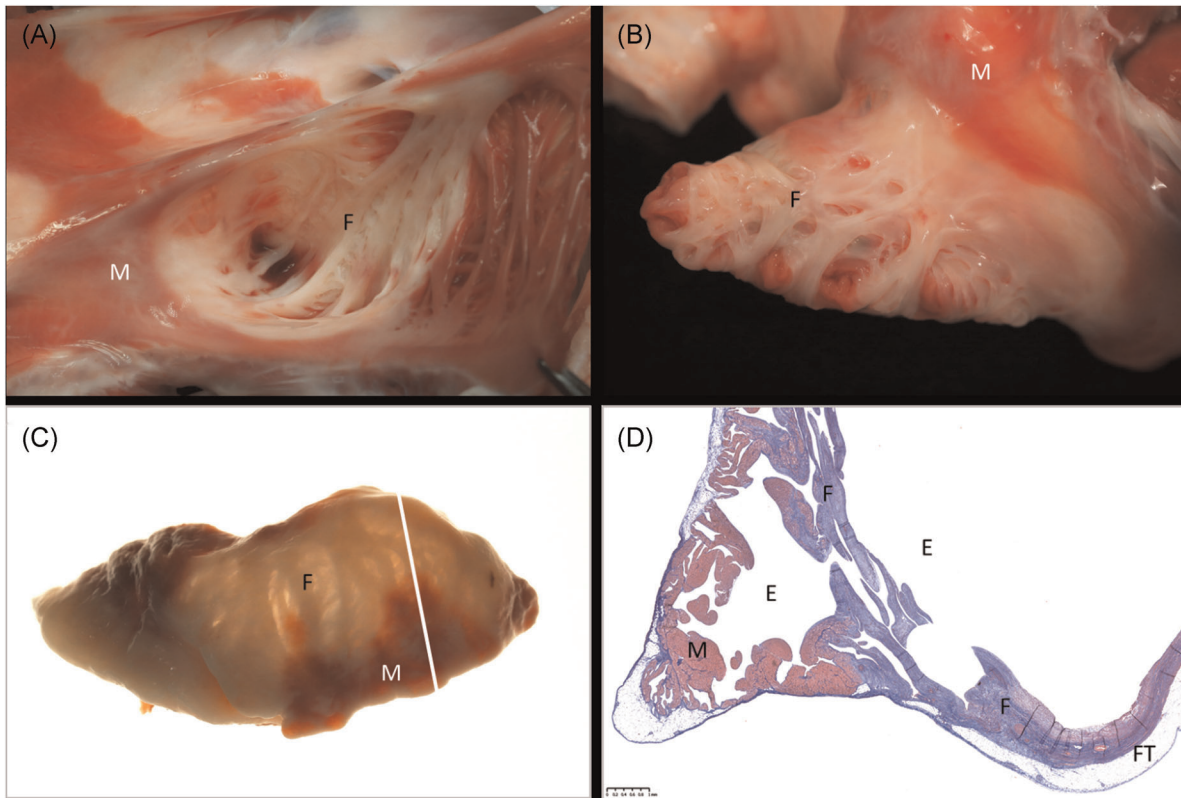


FIGURE 4 Ablation of the RAA. In-situ necropsy finding, enhanced by TTC staining, 4 weeks after high-dose PFA treatment of the RAA when looking into the appendage (A) and after eversion of the appendage to display the endocardium (B). Widespread atrial replacement fibrosis is readily visible under backlight illumination of the same specimen after formalin fixation (C). Histology via Masson's trichrome staining confirms transmural replacement fibrosis in atrial wall segments that were originally made of irregular trabeculation/pectination. White bar in (C) indicates slide origin for (D). E, endothelial side; F, fibrosis after ablation; FT, fat tissue on epicardium (normal); M, muscle (untreated); PFA, pulsed field ablation; RAA, right atrial appendage; TTC, triphenyl tetrazolium chloride

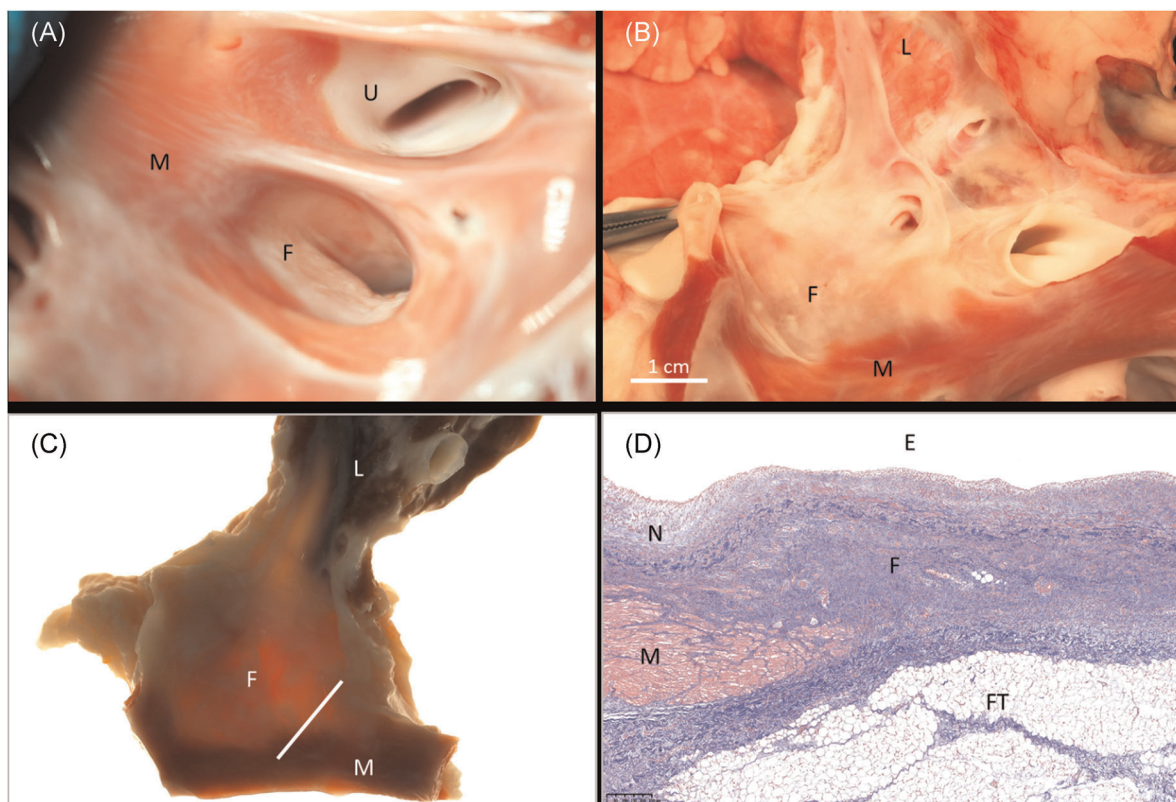


FIGURE 5 Ablation of the RSPV. In-situ necropsy finding, enhanced by TTC staining, 4 weeks after high-dose PFA treatment of the RSPV when looking into its orifice (A) and after longitudinal opening towards the lung (B). There is good evidence of circumferential replacement fibrosis when the same formalin-fixed specimen is examined under backlight illumination (C). Histology via Masson's trichrome staining confirms transmural replacement fibrosis that is covered by neointima and has normal adjacent myocardium (D). White bar in (C) indicates slide origin for (D). E, endothelial side; F, fibrosis after ablation; FT, fat tissue at cardiac base (normal); L, lung; M, muscle (untreated); N, neointima; PFA, pulsed field ablation; RSPV, right superior pulmonary vein; TTC, triphenyl tetrazolium chloride; U, untreated pulmonary vein orifice

Histopathology confirmed that lesions were uniform transmural fibrosis (measuring on average 2.62 ± 1.56 mm, Table 2) that did not include any viable myofiber groups or necrotic sequesters thereof. Of note, when lesion thickness measurements included the depth of the RSPV lesion extending through the adjacent right atrial wall, measured lesion thickness was as great as 6.51 mm (Table 2). Moreover, there was a low degree of local neointima formation, and absence of adventitial fat tissue inflammation (Figure 5D).

3.5 | Postmortem collateral damage profile

At all sites, there was no evidence of stenosis. In total, there was an absence of aneurysms and thrombosis, and no collateral damage of clinical significance was detected via postmortem examination. In particular, there was no damage to any of the RPN where each was juxtaposed to the PFA delivery sites in the SVC and in the RSPV. Specifically, the RPNs showed no histopathological changes, including no Wallerian degeneration, no perineural fibrosis, and no epineural fibrosis (Figure 6A). Moreover, the right side of the diaphragms presented without evidence of neurogenic atrophy.

Careful examination of other collateral tissues revealed mild fibrosis and loss of media myocytes in pulmonary artery branches juxtaposed to high-dose RSPV ablations. There was no epicardial fat tissue inflammation (Figures 4D and 5D) at any PFA sites. Mild adjacent fibrosis was occasionally observed at otherwise normal great vessels or autonomic nerves within ablated myocardial structures (Figure 6B,C).

3.6 | Computer modeling

Numerical modeling results showed an electrical field distribution consistent with a contiguous and transmural lesion forming after the delivery of pulses to using only four placements (Figure 7). The lesion width ranged between 3 and 12 mm on the outer surface of the vein and between 6.5 and 15 mm on the inner surface (Figure 7C,D).

4 | DISCUSSION

Knowing that pulse delivery and ablation strategy is a key component of safety and efficacy, this GLP study sought to evaluate overlapping PFA deliveries in the constrained porcine left atrial

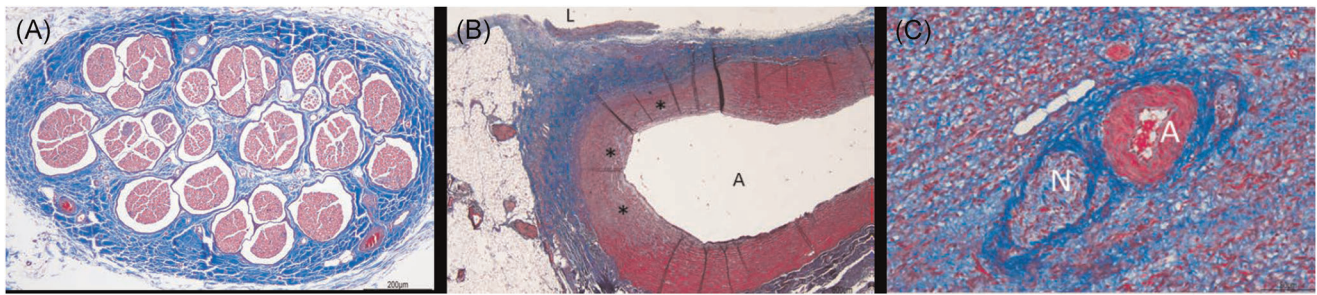
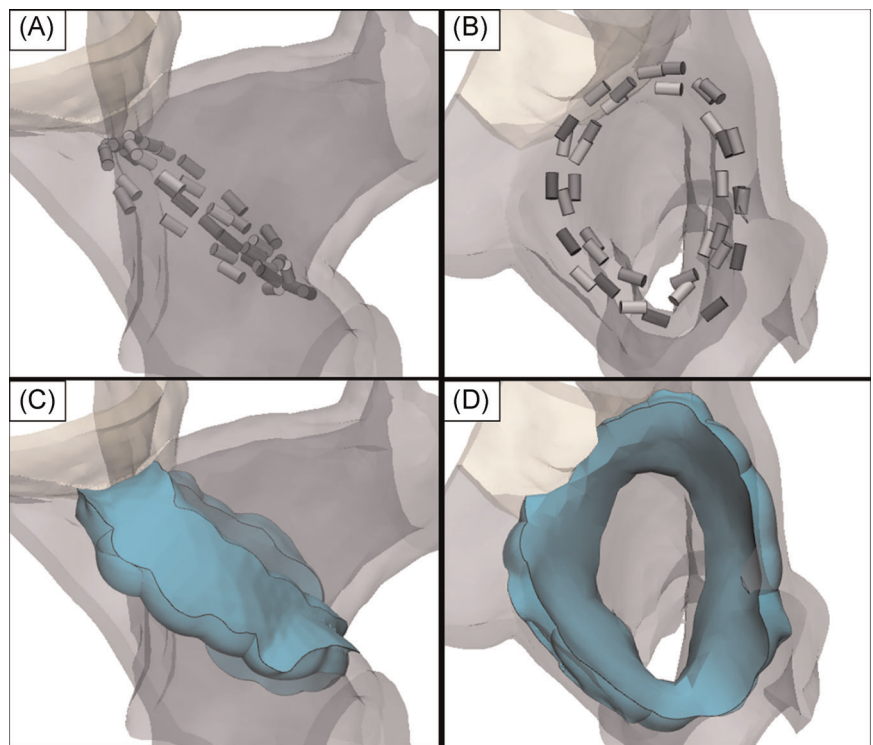


FIGURE 6 (A) Collateral damage profile. Photomicrograph of the right phrenic nerve that illustrates no pathological changes 4 weeks after PFA treatment when low-dose PFA was delivered in the SVC. (B) Histology of a pulmonary artery branch previously juxtaposed to a RSPV ablation and now showing arterial wall remodeling that consisted of mild fibrosis and loss of media myocytes. Photomicrograph from a right atrial appendage with perineural fibrosis and normal appearing artery (C). A, artery; L, lumen; N, nerve; PFA, pulsed field ablation; RSPV, right superior pulmonary vein; SVC, superior vena cava. *Fibrosis and myocyte loss

FIGURE 7 Three-dimensional rendering of the RSPV constructed using contrast enhanced CT images from a single pig. 4 placements of the circular electrode array were positioned at the ostium of the RSPV with the shape of the catheter conforming to the inner surface of the ostium (A and B). Using a conservative field threshold of 550 V/cm and uniform 3 mm tissue thickness, the field isosurfaces predict a contiguous and transmural lesion volume (green) with lesion widths ranging 3–12 mm on the outer surface of the ostium and 6.5–15 mm on the inner surface (C and D). CT, computed tomography; RSPV, right superior pulmonary vein



anatomy with low or high level doses to set the stage for future clinical use. In this study, low- or high-dose PFA deliveries to the SVC, RAA, and RSPV resulted in complete circumferential lesions with replacement fibrosis at four weeks postablation while maintaining a chronic myocardial and collateral tissue safety profile.

This study was a comprehensive 4-week evaluation of a PFA system that was distinct from a prior feasibility preclinical study with an endpoint of two weeks.²⁴ This investigation was performed in parallel with other preclinical studies using the same system, to establish the safety and efficacy of low and high PFA applied voltages (700 and 1500 V) before moving to first-in-human clinical trial with these same voltage levels and PFA system.²⁸ Detailed histopathological analysis of collateral tissues including the phrenic nerve, pulmonary artery, and of non-myelinated autonomic nerves are

offered here for the first time for this system. Also, this is the first PFA study to directly measure local temperature of each individual energy delivery electrode immediately after PFA delivery, with the intent of characterizing the non-thermal nature of PFA deliveries. Although other preclinical studies may have evaluated similar targets, the safety and efficacy of PFA depends on the unique system configuration and electrode array.^{31,32}

4.1 | PFA dosing and chronic lesion characterization

This GLP preclinical study was the first to establish efficacy of overlapping PFA deliveries using two distinct applied voltage levels

on tissues of varying thickness. Transmural lesions were observed in the porcine ablations where PFA was used to create completely circumferential and transmural lesions at all targeted sites while maintaining a favorable safety profile. Specifically, PFA deliveries resulted in complete replacement fibrosis at four weeks without any evidence of thromboembolism or extracardiac damage. Histopathology performed on the ablated porcine tissue did not detect any surviving myofibers nor non-resorbed necrotic myofiber sequesters, further suggesting that effective lesions can be created with PFA with the low and high doses at multiple endocardial structures of variable pre-ablation anatomical architectures.

When delivering RF energy from focal catheters, good electrode-tissue contact force has been proposed as critical for effective lesion formation within the varying structures of the endocardium.^{10–13} The same may not be as true for PFA as evidenced by the lesions created in the RAA, where fibrosis was observed extending from each structure's orifice through a large area of the trabeculated network and muscle bundles preventing uniform electrode-tissue contact. In the relatively smooth walled left atrial anatomy, the electric field model with a conservative IRE threshold level set at 550 V/cm is consistent with complete full-depth circumferential lesions in the RSPV observed in the animal model. The electrical field model predicted a transmural lesion despite imperfect contact at some places along the circular electrode array-to-tissue interface. The lesions were also transmural for the other targeted structures while extracardiac structures adjacent to the ablation were unaffected. These animal and computational modeling results suggest that perfect contact may not be necessary to create a contiguous lesion with the low and high doses.

RF ablation of the SVC has already been shown to be a safe and feasible approach for the treatment of AF, but it may be hampered by the potential thermal injury of collateral tissue (e.g., the proximal phrenic nerve).³³ In the present study, ablations of the SVC using PFA were completely circumferential and transmural without any gaps along the circumference of the lesion. Histology confirmed the grossly observed continuous lesion. This study demonstrated that different doses of PFA result in chronically isolated and ablated structures with this PFA system planned to be used clinically.

4.2 | PFA dosing and collateral injury

Safe and effective dosing of thermal energy has a small but ever present risk of severe complications which has not abated despite new technologies for monitoring contact force and lesion index.^{3,34–38} This study examined excessive deliveries on the same bands of tissue in the RAA and RSPV that produced no injuries to local adjacent endocardial tissue, pulmonary tissues, adjacent nerves, nor esophageal tissue. A favorable safety profile was maintained for both low- and high-doses used in this study, which was aligned with prior preclinical studies.²⁸ No animal experienced intraprocedural ventricular arrhythmia and there were no findings suggestive of charring, collateral tissue injury, or acute thrombus formation

acutely and at 4 weeks postablation (Figures 3–6). These findings continue to support the current hypothesis that intracardiac deliveries of PFA can minimize collateral tissue damage.

Multiple high-dose PFA applications delivered in an overlapping manner between each repositioning of the electrode array at a targeted anatomical site (as shown in Figure 7A,B) on approximately the same band of myocardium in the SVC, RSPV, and RAA demonstrated that even overlapping energy applications to the same tissue did not result in perforation, aneurysm, or collateral damage to tissues, such as the phrenic nerve. No phrenic nerve functional injury or pathologic changes were observed throughout the study, based on histopathological and phrenic nerve stimulation threshold findings. However, non-myelinated autonomic nerves as shown in Figure 6C were occasionally observed to have been injured, which may have clinical significance for the ablation of the ganglionated plexi. The finding that the large myelinated phrenic nerve was unaffected while small autonomic nerves within lesions were observed to have been ablated may have clinical significance if ablation of autonomic ganglia are indeed a factor in the ultimate success of AF ablations but this will require further study.^{39–42} The finding of minor fibrosis in the branch of the pulmonary artery which was adjacent to the multiple overlapping ablations in the RSPV demonstrated that while this was minor and inconsequential focal fibrosis to this non-myocardial tissue, such tissues do have a threshold for injury.

These results regarding the phrenic nerve, autonomic nerves, and pulmonary arteries also lead to the theory that there is a higher IRE threshold in collateral tissues. Another theory is that endocardial tissue in closest contact with the electrodes is exposed to the very highest field strengths, while the tissues beyond the epicardium are exposed to a rapid drop-off in electric field strength. The drop-off in field strength further reduces the chances of collateral tissue damage.^{24,27,43,44} Further modeling and preclinical studies performed systematically with the same PFA system are warranted to better understand field strength drop-off, IRE thresholds and the impact on safety.

Previously, parameters for thermal ablation technologies were evaluated to understand methods of avoiding thermal injury, such as steam pops.^{14,15,45} Electrode temperature rise data collected in this PFA study demonstrated that the mechanism of cardiac ablation from these overlapping PFA deliveries was unlikely to be related to thermal injury since even the high dose PFA deliveries only produced an average temperature rise of about 5°C at 1 s post-pulse train delivery, which is insufficient to produce thermal necrosis of any consequence in the lesion volume.^{46,47} Safety and a non-thermal mechanism are also supported by the lack of thermal deposits on the PFA electrodes after the ablations. The temperature rise measurements, made directly at the electrodes in contact with tissue, demonstrate the non-thermal nature of the technology. Even with the overlapping nature of these deliveries, no thermal damage or sustained temperature rise was observed.

These safety findings are potentially due to the mechanism of action of IRE. Cell death due to electroporation could be the result of apoptosis, depletion of adenosine triphosphate, electroconformational

denaturation of macromolecules, and/or electrolytic pH changes.⁴⁸ Exact mechanisms have not been fully elucidated, but the lack of collateral injury observed during cardiac tissue ablation in this study is consistent with a cell death mechanism that minimizes safety issues commonly associated with RF catheter ablation.

5 | LIMITATIONS

As there are differences between human and porcine anatomy, and potentially differences in susceptibility to electric field exposures, further research is needed to confirm the safety results observed in the study. Due to the GLP safety focus of the study, exit block evaluations were not performed at the time of termination to allow for gross necropsy inspection of undisturbed ablated tissues. Finally, this study was conducted on a small number of animals in a few anatomical structures using either a low or high PFA applied voltage.

6 | CONCLUSION

This study is a chronic comprehensive preclinical GLP study aiming to characterize PFA lesions created in multiple cardiac structures in preparation for the start of a human clinical study. At four weeks post ablation, PFA lesions created in the SVC, RAA, and RSPV were complete, contiguous, transmural and devoid of collateral damage of clinical significance.

ACKNOWLEDGMENTS

The authors would like to acknowledge Louanne Cheever for expert histology support. This study was fully funded by Medtronic Inc.

DISCLOSURES

David Haines, Atul Verma, Damijan Miklavčič, and Bor Kos receive research and consultation funds from Medtronic, Inc. Nicole Kirchof, Noah Barka, Lars Mattison, Matthew Martien, Birce Onal, Brian Howard, and Mark Stewart are employees of Medtronic, Inc.

DATA AVAILABILITY STATEMENT

The data that support the findings of this study are available on request from the corresponding author. The data are not publicly available due to privacy or ethical restrictions.

ORCID

Mark T. Stewart  <https://orcid.org/0000-0003-1717-195X>

Birce Onal  <http://orcid.org/0000-0001-8961-8939>

Atul Verma  <https://orcid.org/0000-0002-1020-9727>

REFERENCES

- Chugh SS, Havmoeller R, Narayanan K, et al. Worldwide epidemiology of atrial fibrillation: a global burden of disease 2010 study. *Circulation*. 2014;129:837-847. <https://doi.org/10.1161/circulationaha.113.005119>
- Morillo CA, Banerjee A, Perel P, Wood D, Jouven X. Atrial fibrillation: the current epidemic. *J Geriatr Cardiol*. 2017;14(3):195-203. <https://doi.org/10.11909/j.issn.1671-5411.2017.03.011>
- Calkins H, Hindricks G, Cappato R, et al. HRS/EHRA/ECAS/APHS/SOLAECE expert consensus statement on catheter and surgical ablation of atrial fibrillation. *Heart Rhythm*. 2017;14:e275-e444. <https://doi.org/10.10106/j.hrthm.2017.05.012>
- Haegeli LM, Calkins H. Catheter ablation of atrial fibrillation: an update. *Eur Heart J*. 2014;35(36):2454-2459. <https://doi.org/10.1093/eurheartj/ehu291>
- Wilber DJ, Pappone C, Neuzil P, et al. Comparison of antiarrhythmic drug therapy and radiofrequency catheter ablation in patients with paroxysmal atrial fibrillation: a randomized controlled trial. *JAMA*. 2010;303(4):333-340. <https://doi.org/10.1001/jama.2009.2029>
- Natale A, Reddy VY, Monir G, et al. catheter ablation with a contact force sensing catheter: results of the prospective, multicenter SMART-AF trial. *J Am Coll Cardiol*. 2014;64(7):647-656. <https://doi.org/10.1016/j.jacc.2014.04.072>
- Chinitz LA, Melby DP, Marchlinski FE, et al. Safety and efficiency of porous-tip contact-force catheter for drug-refractory symptomatic paroxysmal atrial fibrillation ablation: results from the SMART SF trial. *Europace*. 2018;20(Fi_3):f392-f400. <https://doi.org/10.1093/europace/eux264>
- Calkins H, Reynolds MR, Spector P, et al. Treatment of atrial fibrillation with antiarrhythmic drugs or radiofrequency ablation: two systematic literature reviews and meta-analyses. *Circ Arrhythmia Electrophysiol*. 2009;2(4):349-361. <https://doi.org/10.1161/circep.108.824789>
- Ganesan AN, Shipp NJ, Brooks AG, et al. Long-term outcomes of catheter ablation of atrial fibrillation: a systematic review and meta-analysis. *J Am Heart Assoc*. 2013;2(2):e004549. <https://doi.org/10.1161/jaha.112.004549>
- Haldar S, Jarman JW, Panikker S, et al. Contact force sensing technology identifies sites of inadequate contact and reduces acute pulmonary vein reconnection: a prospective case control study. *Int J Cardiol*. 2013;168(2):1160-1166. <https://doi.org/10.1016/j.ijcard.2012.11.072>
- Wittkamp FH, Nakagawa H. RF catheter ablation: Lessons on lesions. Pacing and clinical electrophysiology. *PACE*. 2006;29(11):1285-1297. <https://doi.org/10.1111/j.1540-8159.2006.00533.x>
- Squara F, Latcu DG, Massaad Y, Mahjoub M, Bun SS, Saoudi N. Contact force and force-time integral in atrial radiofrequency ablation predict transmuralty of lesions. *Europace*. 2014;16(5):660-667. <https://doi.org/10.1093/europace/euu068>
- Maurer T, Kuck KH. The quest for durable lesions in catheter ablation of atrial fibrillation—technological advances in radiofrequency catheters and balloon devices. *Expert Rev Med Devices*. 2017;14(8):621-631. <https://doi.org/10.1080/17434440.2017.1358086>
- Aryana A, Baker JH, Espinosa Ginic MA, et al. Posterior wall isolation using the cryoballoon in conjunction with pulmonary vein ablation is superior to pulmonary vein isolation alone in patients with persistent atrial fibrillation: a multicenter experience. *Heart Rhythm*. 2018;15(8):1121-1129. <https://doi.org/10.1016/j.hrthm.2018.05.014>
- Romero J, Michaud GF, Avendano R, et al. Benefit of left atrial appendage electrical isolation for persistent and long-standing persistent atrial fibrillation: a systematic review and meta-analysis. *Europace*. 2018;20(8):1268-1278. <https://doi.org/10.1093/europace/eux372>
- Kotnik T, Rems L, Tarek M, Miklavcic D. Membrane electroporation and electropermeabilization: mechanisms and models. *Annu Rev Biophys*. 2019;48:63-91. <https://doi.org/10.1146/annurev-biophys-052118-115451>
- Campana LG, Edhemovic I, Soden D, et al. Electrochemotherapy - Emerging applications technical advances, new indications,

- combined approaches, and multi-institutional collaboration. *Eur J Surg Oncol*. 2019;45(2):92-102. <https://doi.org/10.1016/j.ejso.2018.11.023>
18. Neumann E, Kakorin S. Membrane electroporation: chemical thermodynamics and flux kinetics revisited and refined. *Eur Biophys J*. 2018;47(4):373-387. <https://doi.org/10.1007/s00249-018-1305-3>
 19. Jiang C, Davalos RV, Bischof JC. A review of basic to clinical studies of irreversible electroporation therapy. *IEEE Trans Biomed Eng*. 2015; 62(1):4-20. <https://doi.org/10.1109/tbme.2014.2367543>
 20. Miklavčič D, Mali B, Kos B, Heller R, Serša G. Electrochemotherapy: from the drawing board into medical practice. *Biomed Eng Online*. 2014;13(1):29. <https://doi.org/10.1186/1475-925x-13-29>
 21. Garcia PA, Davalos RV, Miklavcic D. A numerical investigation of the electric and thermal cell kill distributions in electroporation-based therapies in tissue. *PLOS One*. 2014;9(8):e103083. <https://doi.org/10.1371/journal.pone.0103083>
 22. Scheffer HJ, Nielsen K, de Jong MC, et al. Irreversible electroporation for nonthermal tumor ablation in the clinical setting: a systematic review of safety and efficacy. *J Vasc Interventional Radiol*. 2014;25(7):997-1011. <https://doi.org/10.1016/j.jvir.2014.01.028>
 23. Lavee J, Onik G, Mikus P, Rubinsky B. A novel nonthermal energy source for surgical epicardial atrial ablation: irreversible electroporation. *Heart Surg Forum*. 2007;10(2):E162-E167. <https://doi.org/10.1532/hsf98.20061202>
 24. Stewart MT, Haines DE, Verma A, et al. Intracardiac pulsed field ablation: proof of feasibility in a chronic porcine model. *Heart Rhythm*. 2019;16(5):754-764. <https://doi.org/10.1016/j.hrthm.2018.10.030>
 25. Reddy VY, Koruth J, Jais P, et al. Ablation of atrial fibrillation with pulsed electric fields: an ultra-rapid, tissue-selective modality for cardiac ablation. *JACC Clin Electrophysiol*. 2018;4(8):987-995. <https://doi.org/10.1016/j.jacep.2018.04.005>
 26. Wittkamp FHM, van Es R, Neven K. Electroporation and its relevance for cardiac catheter ablation. *JACC Clin Electrophysiol*. 2018; 4(8):977-986. <https://doi.org/10.1016/j.jacep.2018.06.005>
 27. Sugrue A, Maor E, Ivorra A, et al. Irreversible electroporation for the treatment of cardiac arrhythmias. *Expert Rev Cardiovasc Ther*. 2018; 16(5):349-360. <https://doi.org/10.1080/14779072.2018.1459185>
 28. Howard B, Haines DE, Verma A, et al. Reduction in pulmonary vein stenosis and collateral damage with pulsed field ablation compared with radiofrequency ablation in a canine model. *Circ Arrhythmia Electrophysiol*. 2020;13(9):e008337. <https://doi.org/10.1161/circep.120.008337>
 29. Sel D, Cukjati D, Batiuskaite D, Slivnik T, Mir LM, Miklavcic D. Sequential finite element model of tissue electroporation. *IEEE Trans Biomed Eng*. 2005;52(5):816-827. <https://doi.org/10.1109/tbme.2005.845212>
 30. Pucihar G, Krmelj J, Reberšek M, Napotnik TB, Miklavčič D. Equivalent pulse parameters for electroporation. *IEEE Trans Biomed Eng*. 2011;58(11):3279-3288. <https://doi.org/10.1109/tbme.2011.2167232>
 31. Koruth J, Kuroki K, Iwasawa J, et al. Preclinical evaluation of pulsed field ablation: electrophysiological and histological assessment of thoracic vein isolation. *Circ Arrhythmia Electrophysiol*. 2019;12(12): e007781. <https://doi.org/10.1161/circep.119.007781>
 32. Sugrue A, Vaidya V, Witt C, et al. Irreversible electroporation for catheter-based cardiac ablation: a systematic review of the pre-clinical experience. *J Interventional Cardiac Electrophysiol*. 2019;5(3): 251-265. <https://doi.org/10.1007/s10840-019-00574-3>
 33. Li JY, Jiang JB, Zhong GQ, Ke HH, He Y. Comparison of empiric isolation and conventional isolation of superior vena cava in addition to pulmonary vein isolation on the outcome of paroxysmal atrial fibrillation ablation. *Int Heart J*. 2017;58(4):500-505. <https://doi.org/10.1536/ihj.16-460>
 34. Zhou X, Lv W, Zhang W, et al. Impact of contact force technology on reducing the recurrence and major complications of atrial fibrillation ablation: a systematic review and meta-analysis. *Anatol J Cardiol*. 2017;17(2):82-91. <https://doi.org/10.14744/AnatolJCardiol.2016.7512>
 35. Shurrab M, Di Biase L, Briceno DF, et al. Impact of contact force technology on atrial fibrillation ablation: a meta-analysis. *J Am Heart Assoc*. 2015;4(9):e002476. <https://doi.org/10.1161/jaha.115.002476>
 36. De Potter T, Van Herendael H, Balasubramaniam R, et al. Safety and long-term effectiveness of paroxysmal atrial fibrillation ablation with a contact force-sensing catheter: real-world experience from a prospective, multicentre observational cohort registry. *Europace*. 2018;20(Fi_3):f410-f418. <https://doi.org/10.1093/europace/eux290>
 37. Phlips T, Taghji P, El Haddad M, Wolf M, Knecht S, Vandekerckhove Y, Tavernier R, Duytschaever M. Improving procedural and one-year outcome after contact force-guided pulmonary vein isolation: the role of interlesion distance, ablation index, and contact force variability in the 'CLOSE'-protocol. *Europace*. 2018;20(Fi_3):f419-f427. <https://doi.org/10.1093/europace/eux376>
 38. Begg GA, O'Neill J, Sohaib A, et al. Multicentre randomised trial comparing contact force with electrical coupling index in atrial flutter ablation (VERISMART trial). *PLOS One*. 2019;14(4): e0212903. <https://doi.org/10.1371/journal.pone.0212903>
 39. Kampaktsis PN, Oikonomou EK, Cheung DYC, JW. Efficacy of ganglionated plexi ablation in addition to pulmonary vein isolation for paroxysmal versus persistent atrial fibrillation: a meta-analysis of randomized controlled clinical trials. *J Interventional Cardiac Electrophysiol*. 2017;50(3):253-260. <https://doi.org/10.1007/s10840-017-0285-z>
 40. Scherlag BJ, Nakagawa H, Patterson E, Jackman WM, Lazzara R, Po SS. The autonomic nervous system and atrial fibrillation: the roles of pulmonary vein isolation and ganglionated plexi ablation. *J Atr Fibrillation*. 2009;2(2):177. <https://doi.org/10.4022/jafib.177>
 41. Zhou Q, Hou Y, Yang S. A meta-analysis of the comparative efficacy of ablation for atrial fibrillation with and without ablation of the ganglionated plexi. *Pacing Clin Electrophysiol*. 2011;34(12): 1687-1694. <https://doi.org/10.1111/j.1540-8159.2011.03220.x>
 42. Madhavan M, Venkatachalam KL, Swale MJ, et al. Novel percutaneous epicardial autonomic modulation in the canine for atrial fibrillation: results of an efficacy and safety study. *Pacing Clin Electrophysiol*. 2016;39(5):407-417. <https://doi.org/10.1111/pace.12824>
 43. Neven K, van Es R, van Driel V, et al. Acute and long-term effects of full-power electroporation ablation directly on the Porcine esophagus. *Circ Arrhythmia Electrophysiol*. 2017;10(5). <https://doi.org/10.1161/circep.116.004672>
 44. van Driel VJ, Neven KG, van Wessel H, et al. Pulmonary vein stenosis after catheter ablation: electroporation versus radiofrequency. *Circ Arrhythmia Electrophysiol*. 2014;7(4):734-738. <https://doi.org/10.1161/circep.113.001111>
 45. Iles TL, Quallich SG, Iazzo PA. Identification of radiofrequency ablation catheter parameters that may induce intracardiac steam pops: direct visualization of elicitation in reanimated Swine hearts. *J Cardiovasc Transl Res*. 2019;12(3):250-256. <https://doi.org/10.1007/s12265-018-9844-7>
 46. Haines DE. The biophysics of radiofrequency catheter ablation in the heart: the importance of temperature monitoring. *Pacing Clin Electrophysiol*. 1993;16(3 Pt 2):586-591. <https://doi.org/10.1111/j.1540-8159.1993.tb01630.x>

47. Haines DE, Watson DD, Verow AF. Electrode radius predicts lesion radius during radiofrequency energy heating. Validation of a proposed thermodynamic model. *Circulation research*. 1990;67(1):124-129. <https://doi.org/10.1161/01.res.67.1.124>
48. Polajzer T, Jarm T, Miklavcic D. Analysis of damage-associated molecular pattern molecules due to electroporation of cells in vitro. *Radiol Oncol*. 2020;54(3):317-328. <https://doi.org/10.2478/raon-2020-0047>

How to cite this article: Stewart MT, Haines DE, Miklavčič D, et al. Safety and chronic lesion characterization of pulsed field ablation in a Porcine model. *J Cardiovasc Electrophysiol*. 2021; 32:958–969. <https://doi.org/10.1111/jce.14980>